

Momentum distribution in heavy deformed nuclei: Role of effective massV. O. Nesterenko,^{1,2} V. P. Likhachev,² P.-G. Reinhard,³ V. V. Pashkevich,¹ W. Kleinig,^{1,4} and J. Mesa²
¹*Bogoliubov Laboratory of Theoretical Physics, Joint Institute for Nuclear Research 141980, Dubna, Moscow Region, Russia*²*Instituto de Física, Universidade de São Paulo, São Paulo, Brazil*³*Institut für Theoretische Physik, Universität Erlangen, D-91058 Erlangen, Germany*⁴*Technische Universität Dresden, Institut für Analysis, Dresden, D-01062, Germany*

(Received 16 July 2004; published 17 November 2004)

The impact of nuclear deformation and effective mass m^*/m on the momentum distributions (MD) of occupied proton states in ^{238}U is investigated in the self-consistent Skyrme-Hartree-Fock (SHF) scheme with parameterizations SkT6, SkM*, SLy6, and SkI3 as well as with the phenomenological Woods-Saxon (WS) shell model. The deformation effect turns out to be significant in the low-momentum domain of $K^\pi=1/2^\pm$ states (mainly of those lying near the Fermi surface) and negligible for other states. The most remarkable result is that all Skyrme parameterizations (with essentially different m^*/m) and the WS potential give very similar MD. This means that the value of effective mass, although crucial for single-nucleon spectra, is not important for the spatial shape of the wave functions and thus for the MD. For the description of MD at $0 \leq k \leq 300 \text{ MeV}/c$, one may use any single-particle scheme fitted properly to the global ground state properties.

DOI: 10.1103/PhysRevC.70.057304

PACS number(s): 21.60.-n, 21.10.Ft, 21.30.Fe, 27.90.+b

The momentum distributions (MD) of nucleons in nuclei provide a basic observable carrying important information on the single-particle structure of nuclei (see Ref. [1] and references therein). We will consider here two, yet little explored, aspects of the theoretical description of MD. The first aspect is the effect of nuclear deformation on MD. The deformation mixes different spherical components in the single-particle wave functions [2] and thus can affect MD. At the same time, the single-particle MD extracted from $(e, e'p)$ and other reactions with deformed nuclei are often angular averaged [3], which somewhat smears out the deformation effects. The question is how strong is the remaining effect? Investigations [4,5] hint that there are some states in the spectrum for which the deformation effect is essential. The second aspect concerns the self-consistent Skyrme-Hartree-Fock (SHF) approaches [6] coming now into the focus of MD studies. The Skyrme forces allow for nonunit values of the effective mass m^*/m , which is known to have a dramatic effect on single-particle spectra [7,8]. But its influence on MD of individual states is still unclear.

We will consider here the axially deformed actinide nucleus ^{238}U as test case. The heavier the nucleus, the denser its single-particle spectrum, and thus the better the conditions for the deformation mixing. So, actinides promise to deliver the strongest deformation effects. For exploring the effects in self-consistent models, we will use four Skyrme parameterizations (SkT6 [9], SkM* [10], SLy6 [11], and SkI3 [12]) with essentially different effective masses m^*/m . For reasons of comparison, we will also check with results from the phenomenological Woods-Saxon (WS) potential [13].

A few words on the calculational schemes: In the WS, the deformed shape is described by the Cassini ovaloids allowing us to parameterize elongation (=quadrupole) and hexadecapole deformation [13]. The ground state deformation is found by minimizing the total energy. We use the standard set of the WS parameters [14] slightly modified for actinides [15]. The single-particle wave functions are expanded in the

Nilsson basis involving 21 shells. The SHF calculations employ a coordinate-space grid with cylindrical coordinates [16]. Although the Skyrme forces SkT6, SkM*, SLy6, and SkI3 are fitted with a different bias, they all provide a good overall description of nuclear bulk properties and are equally suitable for heavy deformed nuclei (for an extensive review see Ref. [17]). For our aims, it is important that these four forces cover different values of the effective mass m^*/m , (see Table I).

The bare G matrix theory results in $m^*/m=0.7$ [18]. The same value is obtained from empirical data for the levels far beyond the Fermi energy, $|E-E_F| \geq 20 \text{ MeV}$, in Ref. [7]. The effective masses $m^*/m < 1$ are known to stretch the single-particle spectra [7,8], making them dilute as compared to the experimental data. After taking into account the correlation effects, the spectra should be more compressed and come closer to the experimental level density near the Fermi surface. Actual Skyrme parameterizations are developed with m^*/m as a fitting parameter varied in a reasonable interval $0.6 < m^*/m < 1$. The actual value for m^*/m depends on the preferences of observables in the fit. The giant quadrupole resonance is best fitted with $m^*/m \approx 0.8$, the value as in SkM*. Nuclear surface properties seem to drive to the lower

TABLE I. Effective masses (m^*/m) for Skyrme forces, quadrupole moments (Q_2), Fermi energies (E_F), and energies of the lowest (E_0) proton single-particle levels in ^{238}U . Experimental estimations for the quadrupole moment in ^{238}U lie in the interval $Q_2=11.1-11.3 \text{ b}$ [19,20].

Potential	m^*/m	Q_2 (b)	E_F (MeV)	E_0 (MeV)
WS	—	11.66	-6.63	-33.69
SkT6	1.00	11.10	-6.48	-32.75
SkM*	0.79	11.11	-6.17	-39.80
SLy6	0.69	11.06	-7.25	-43.12
SkI3	0.58	10.89	-7.19	-48.53

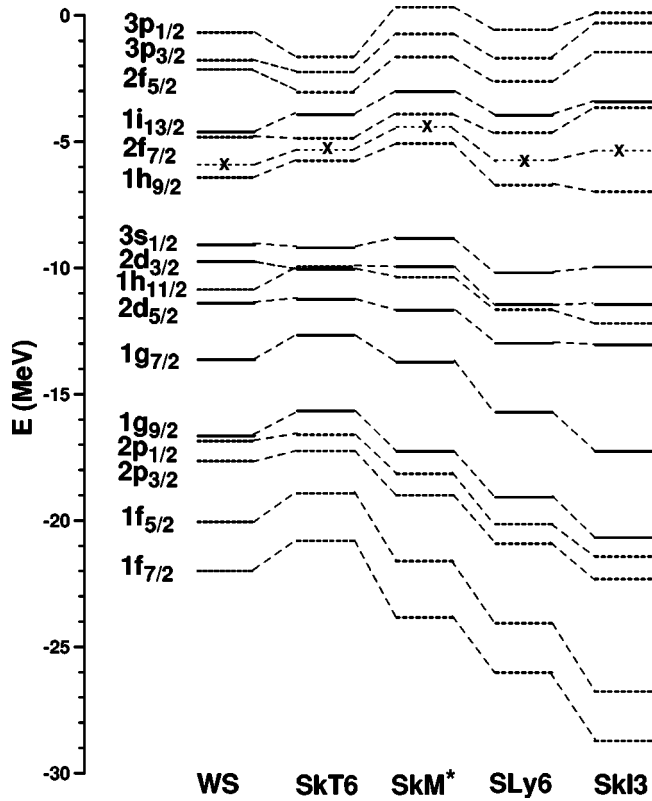


FIG. 1. WS and SHF proton single-particle spectra in ^{238}U at zero deformation (spherical limit). The levels of the positive and negative parity are depicted by solid and dotted lines, respectively. As a guide for the eyes, identical levels are connected by dashed lines. The chemical potentials are indicated by dotted lines with crosses.

values found in SLy6 and SkI3. A bias on nuclear energies complies well with $m^*/m \approx 1$. WS, Nilsson, and other phenomenological potentials employ a “trivial” kinetic energy, i.e., $m^*/m = 1$. Thus they should in general give spectra close to the Skyrme ones with $m^*/m \sim 1$.

Basic ground state properties for the different models are shown in Table I. The WS potential and all SHF parameterizations give a reasonable quadrupole moment and Fermi energy for ^{238}U . At the same time, they yield different spectral stretching (defined as the difference, $|E_F - E_0|$, between the Fermi energy and the energy of the lowest single-particle level). The stretching ranges from 26 to 41 MeV and grows with decreasing the effective mass. SkT6 with $m^*/m = 1$ gives an average spectral density close to the WS one.

The dependence of the proton spectra on the m^*/m is illustrated in Fig. 1. For a more transparent analysis, the levels are presented in the spherical limit. This avoids the complexity caused by the deformation splitting and thus concentrates on the essential trends. The figure clearly shows the stretching of the single-particle spectra with decreasing m^*/m . While the Fermi energies remain basically at the similar position, the hole levels steadily dive deeper from SkT6 with $m^*/m = 1.00$ to SkI3 with $m^*/m = 0.58$. In agreement with Ref. [7], the main stretching effect takes place for the spectra far from the Fermi energy. The spectra near the Fermi energy also show changes but not so strong and regular.

The MD are computed as follows: In cylindrical coordinates (r, z, ϕ) , the single-particle wave function of the state α is

$$\psi_\alpha(\mathbf{r}) = \sum_{\sigma=\pm 1} R_\alpha^{(\sigma)}(r, z) e^{im_\alpha^{(\sigma)}\phi} \chi_\sigma, \quad (1)$$

where the label $\alpha = K^\pi [Nn_z\Lambda]$ includes the exact quantum numbers K^π (total angular momentum along the axial symmetry axis and parity) and the asymptotic Nilsson quantum numbers $[Nn_z\Lambda]$. Further, $\sigma = \pm 1/2$ and $m^{(\sigma)} = K - \sigma$ are the spin and orbital momentum projections, respectively. In momentum space (k_r, k_z, k_ϕ) , the density reads

$$n_\alpha(\mathbf{k}) = |\psi_\alpha(\mathbf{k})|^2 = \sum_{\sigma=\pm 1} |\tilde{R}_\alpha^{(\sigma)}(k_r, k_z)|^2, \quad (2)$$

where $\psi_\alpha(\mathbf{k})$ is the Fourier-transformed single-particle wave function. In the WS potential, the wave functions are expanded in the Nilsson basis whose Fourier transformation is done analytically (for more details see, e.g., Ref. [4]). In SHF, the Fourier transformation is done directly from coordinate space into momentum space using the basis function appropriate for cylindrical coordinates, namely plane waves along z direction and Bessel functions $J_{m_\alpha^{(\sigma)}}(k_r, r)$ in radial direction (see Ref. [21] for more details).

As is usually done in $(e, e'p)$ calculations, we average Eq. (2) over the nuclear symmetry axis direction:

$$n_\alpha(k) = \frac{1}{2} \int_0^\pi d\theta \sin \theta n_\alpha(k_r, k_z), \quad (3)$$

where $k_r = k \sin \theta$ and $k_z = k \cos \theta$. Of course, this averaging smooths the deformation effect. However, we consider the averaged MD (3) since this value is often used in the analysis of the knock-out reactions. And it is important to understand how strong deformation effects remain in MD after the averaging by all the orientations.

It is also worth noting that in general single-particle models are not well suited to describe MD because of the important contributions from short- and long-range correlations [1]. However, these perturbing effects take place mainly in the high-momentum domain with $k > k_F \approx 1.3 \text{ fm}^{-1} \approx 260 \text{ MeV}/c$ while we will focus on MD at low k , where the single-particle models are still appropriate.

Figure 2 compares the MD from SkM* calculated at the equilibrium shape and in the spherical limit for a representative set of occupied proton states. Both deeply and slightly bound states are involved. The deep hole states include $1/2^- [330]$ and $1/2^- [301]$ (with the single-particle energies -26.5 and -17.2 MeV , respectively). The other six states lie near the Fermi energy. As is discussed below, they are expected to deliver the most pronounced deformation effects and thus we pay them more attention. In the spherical limit, the number of maxima in the MD profile for the state nlj is equal to the number of radial nodes n . Hence, the deformation effects can be easily spotted by looking at an increasing number of the maxima and/or an essential redistribution of the strength between the maxima. We present here the SkM* results though, as is discussed below, other Skyrme parameterization might be used as well.

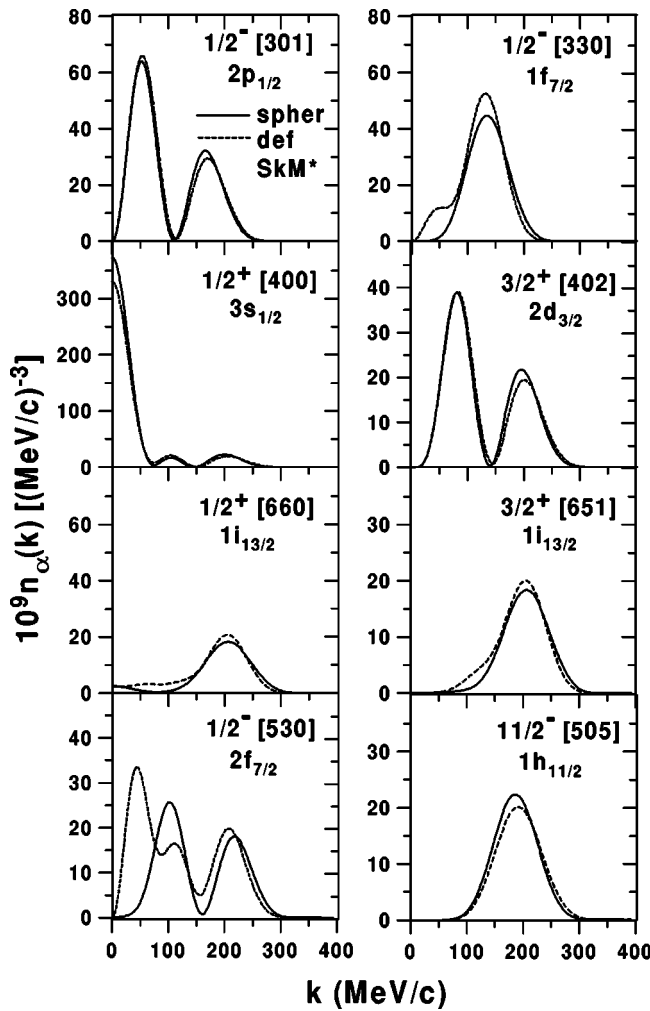


FIG. 2. Momentum distributions for occupied proton states in ^{238}U calculated with SkM* in the spherical limit (solid line) and at the equilibrium deformations (dashed line). The spherical ancestors are indicated for every state.

Figure 2 shows some general deformation effects: (i) The lower the K quantum number, the stronger the deformation effect, see e.g., the $K=1/2$ states $1/2^- [330]$ and $1/2^- [530]$. This follows from the fact that spherical configurations with low K have in general a denser spectrum than those with high K , which favors the mixing low- K states due to the deformation. The exceptions (e.g., $1/2^- [301]$) mainly concern deeply bound states whose mixing is often suppressed due to a rather dilute spectrum. (ii) The levels near the Fermi energy are more affected by the deformation because they reside in a region of higher spectral density. (iii) The deformation usually results in a shift of the MD strength to lower momenta. Note that the normalization condition $\int n_\alpha(k) k^2 dk = 1$ carries a weight k^2 and so even a small modification of MD at high k may cause considerable changes at low k . As a result, the low- k domain is most sensitive to deformation (see also the discussion on $K^\pi=1/2^+$ states in Ref. [5]).

Altogether, one may conclude that in heavy nuclei the $K=1/2$ states in the vicinity of the Fermi energy are most promising for displaying the deformation effect in MD. In

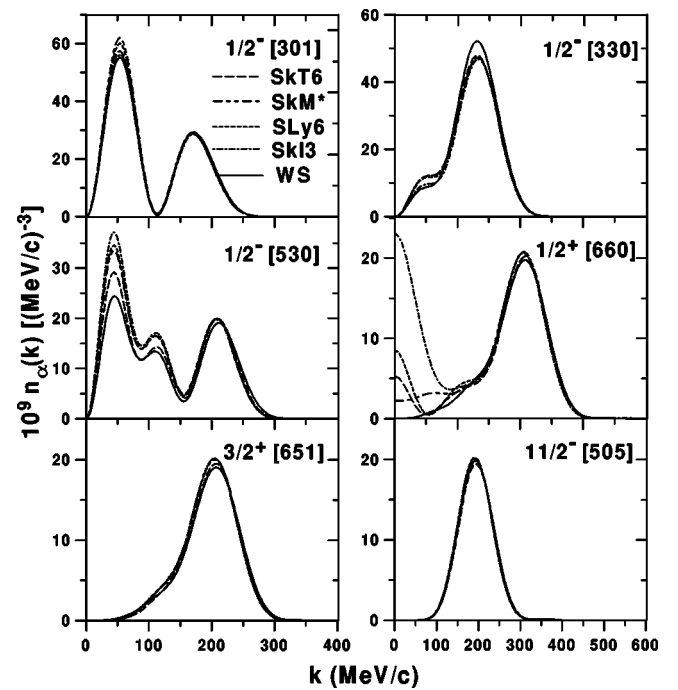


FIG. 3. Proton momentum distributions in ^{238}U calculated with WS (solid line) and Skyrme potentials SKT6 (dashed line), SkM* (dashed-double-dotted line), SLy6 (dotted line), and SKI3 (dashed-dotted line).

deeply bound states, even if they are influenced by the deformation, the momentum distributions should be considerably smeared by correlations, thus hiding, to a large extent, the deformation mixing. The only chance for deeply bound states to exhibit in experiment the deformation effects is offered by the $K^\pi=1/2^+$ states, where the deformation-induced $l=0$ strength is strictly localized at $k=0$ and so can in principle be distinguished from the $l \neq 0$ patterns [5].

Figure 3 compares MD for WS and four different Skyrme forces (SKT6, SkM*, SLy6, and SKI3). We see rather good agreement between WS and SHF distributions. The modest differences mainly take place at low k where deformation effects are most strong. This result somewhat deviates from that in Ref. [5] where the deformation effects in the WS potential were overestimated because of the insufficiently accurate treating of the WS wave functions in the momentum space. It is worth noting that the calculations [4] for Ne and Nd also display rather modest differences between phenomenological (Nilsson) and Skyrme (SIII) MD.

The most striking result displayed in Fig. 3 is that, in spite of the very different effective masses, all the Skyrme parameterizations give very similar MD. The deviations are about invisible at high momenta for all the states and at all momenta for the states with high K . Even for deep hole states $1/2^- [301]$ and $1/2^- [330]$, the MD are about the same. The state $1/2^- [530]$ with the maximal deformation effect (see Fig. 2) also demonstrates rather small deviations. The only strong difference takes place at low k in $1/2^+ [660]$. However, this case is very specific and reflects the considerable mixing of $1/2^+ [660]$ and $1/2^+ [400]$. Just because of the $1/2^+ [400]$ admixture with its dominant $3s_{1/2}$ component, the

state $1/2^+[660]$ acquires a jump at $k=0$. The mixing $1/2^+[660]$ and $1/2^+[400]$ levels is caused by their pseudocrossing at the equilibrium deformation. The states exhibiting the pseudocrossing are usually very sensitive to details of the single-particle scheme and in this sense the state $1/2^+[660]$ is an exception from the general picture. So, we may conclude that value of the effective mass, being crucial for the description of the spectra, turns out to be irrelevant for the momentum distributions.

The remarkable insensitivity of MD to the effective mass means that single-particle wave functions are much less sensitive to m^*/m than the single-particle spectra. Moreover, together with the similarity of MD from different potentials (Nilsson, WS, SHF), this result signifies a general robustness of MD at low k . This may be understood when realizing that MD at low k are determined by the structure of the wave functions that are mainly specified by the orbital moment and number of nodes of the dominant components. All the relevant single-particle potentials evidently keep this structure in the spherical limit. In deformed nuclei, the different models should reproduce the nuclear quadrupole moment and then their eigenfunctions should have a similar composition of angular momentum components, thus giving similar MD. It is essential that all the reasonable models are fitted to overall extensions of the system. Adjusting the spatial extensions seems to determine at once the extensions of all single-

particle states, which in turn, fixes the position of nodes and maxima in the momentum space distribution. Finally, we may conclude that any single-particle potential (phenomenological or self-consistent) that reproduces the basic ground state properties should accurately describe momentum distributions of individual states in the momentum domain $0 \leq k \leq 300 \text{ MeV}/c$ (with exception of the level pseudocrossing cases).

In summary, we have studied the effect of deformation and effective mass in the averaged momentum distributions of heavy deformed nuclei. The main deformation effects were found in the low-momentum domain of $K^\pi = 1/2^\pm$ states near the Fermi surface. The effective mass is found to have practically no influence on the MD although it modifies strongly the single-nucleon spectra. Results from all Skyrme forces turn out to be similar to those from a Woods-Saxon model. It seems that, for the description of MD at low k (and the subsequent inputs for knock-out reactions), one can use any well fitted Skyrme or phenomenological potentials. This simplifies the analysis of knock-out reactions.

We thank Professor A.N. Antonov and Professor S. Frauendorf for fruitful discussions. This work was supported by FAPESP Grant No. 2001/06082-1, Germany-BLTP JINR (Heisenberg-Landau) and Bundesministerium für Bildung und Forschung (BMBF), Project No. 06 ER 808.

-
- [1] A. N. Antonov, P. E. Hodgson, and I. Zh. Petkov, *Nucleon Correlations in Nuclei* (Springer-Verlag, Berlin, Heidelberg, 1993).
- [2] F. A. Gareev *et al.*, Nucl. Phys. **A171**, 134 (1971).
- [3] V. P. Likhachev *et al.*, Phys. Rev. C **65**, 044611 (2002).
- [4] J. A. Caballero and E. Moya de Guerra, Nucl. Phys. **A509**, 117 (1990); E. Moya de Guerra *et al.*, *ibid.* **A529**, 68 (1991).
- [5] V. O. Nesterenko *et al.*, J. Phys. G **29**, L37 (2003).
- [6] T. H. R. Skyrme, Philos. Mag. **1**, 1043 (1956); D. Vauterin and D. M. Brink, Phys. Rev. C **5**, 626 (1972).
- [7] C. Mahaux *et al.*, Phys. Rep. **120**, 1 (1985).
- [8] B. A. Brown, Phys. Rev. C **58**, 220 (1998).
- [9] F. Tondeur *et al.*, Nucl. Phys. **A420**, 297 (1984).
- [10] J. Bartel *et al.*, Nucl. Phys. **A386**, 79 (1982).
- [11] E. Chabanat *et al.*, Nucl. Phys. **A643**, 441(E) (1998).
- [12] P.-G. Reinhard and H. Flocard, Nucl. Phys. **A584**, 467 (1995).
- [13] V. V. Pashkevich, Nucl. Phys. **A169**, 275 (1971).
- [14] V. A. Chepurnov, Sov. J. Nucl. Phys. **6**, 696 (1968).
- [15] F. Garcia *et al.*, Eur. Phys. J. A **6**, 49 (1999).
- [16] P.-G. Reinhard (unpublished).
- [17] M. Bender, P.-H. Heenen, and P.-G. Reinhard, Rev. Mod. Phys. **75**, 121 (2003).
- [18] V. Bernard and N. Van Giai, Nucl. Phys. **A348**, 75 (1980).
- [19] E. N. Shurshikov, Nucl. Data Sheets **53**, 601 (1988).
- [20] V. G. Soloviev, *Theory of Complex Nuclei* (Pergamon Press, Oxford, 1976).
- [21] V. O. Nesterenko *et al.*, nucl-th/0407048.